

# Towards Language-guided Visual Recognition via Dynamic Convolutions

Gen Luo<sup>1</sup>, Yiyi Zhou<sup>1,2\*</sup>, Xiaoshuai Sun<sup>1,2</sup>, Yongjian Wu<sup>3</sup>, Yue Gao<sup>4</sup> and Rongrong Ji<sup>1,2</sup>

<sup>1</sup>Key Laboratory of Multimedia Trusted Perception and Efficient Computing, Ministry of Education of China, Xiamen University, 361005, P.R. China..

<sup>2</sup>Institute of Artificial Intelligence, Xiamen University, 361005, China.

<sup>3</sup>Youtu Lab, Tencent.

<sup>4</sup>Software School of Tsinghua University.

\*Corresponding author(s). E-mail(s): [zhouyiyi@xmu.edu.cn](mailto:zhouyiyi@xmu.edu.cn);

Contributing authors: [luogen@stu.xmu.edu.cn](mailto:luogen@stu.xmu.edu.cn);  [{zhouyiyi, xssun, rrji}@xmu.edu.cn](mailto:{zhouyiyi, xssun, rrji}@xmu.edu.cn); [littlekenwu@tencent.com](mailto:littlekenwu@tencent.com); [gaoyue@tsinghua.edu.cn](mailto:gaoyue@tsinghua.edu.cn);

## Abstract

In this paper, we are committed to establishing a unified and end-to-end multi-modal network via exploring language-guided visual recognition. To approach this target, we first propose a novel multi-modal convolution module called *Language-guided Dynamic Convolution* (LaConv). Its convolution kernels are dynamically generated based on natural language information, which can help extract differentiated visual features for different multi-modal examples. Based on the LaConv module, we further build a fully language-driven convolution network, termed as *LaConvNet*, which can unify the visual recognition and multi-modal reasoning in one forward structure. To validate LaConv and LaConvNet, we conduct extensive experiments on seven benchmark datasets of three vision-and-language tasks, *i.e.*, visual question answering (VQA), referring expression comprehension (REC) and segmentation (RES). The experimental results not only show the competitive or better performance of LaConvNet against existing multi-modal networks, but also witness the merits of LaConvNet as an unified structure, including compact network, low computational cost and high generalization ability. Our source code is released in SimREC project: <https://github.com/luogen1996/LaConvNet>.

**Keywords:** Referring Expression Comprehension, Visual Reasoning, Vision and Language

## 1 Introduction

In recent years, the rapid development of joint vision-language study have been supported by a flurry of benchmark datasets [3, 17, 23, 30, 34, 36, 48, 56, 64] and methods [1, 28, 29]. The latest research trend [29, 57, 58, 64, 71] has gone beyond a simple understanding of multi-modal

information [60, 66, 95], and focused on more advanced cognitive tasks, such as visual reasoning [30, 34, 48, 96], visual question answering (VQA) [3, 17, 30, 34, 41, 97], and referring expression comprehension (REC) [23, 36, 48, 56, 65].

To accomplish these tasks, most existing vision-and-language (VL) systems adopt a modular structure. As shown in Fig. 1 (a), a

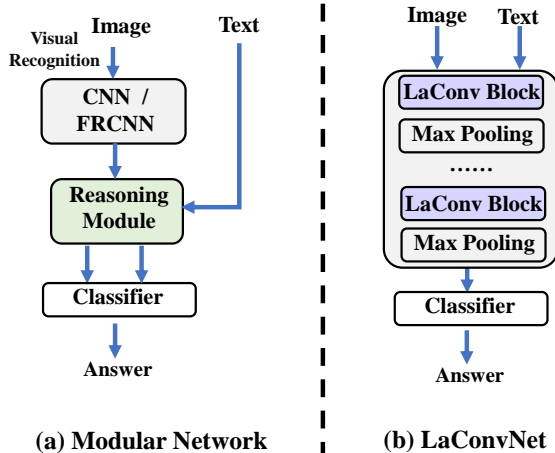


**Fig. 1** Comparison between the conventional modular network and our unified model. The proposed LaConv block can combine visual recognition and multi-modal interaction into one processing step. Based on it, we build a unified and end-to-end network called LaConvNet.

typical VL system often uses a visual backbone, *e.g.*, ResNet [18] or FasterRCNN [69], to extract the features of the input image, based on which another inference network is deployed to model cross-modal interactions. This long-popular paradigm has achieved great success in various VL tasks [3, 17, 23, 34], but has been also criticized for its excessive parameters and high computational overhead [39, 82, 83].

In contrast to this modular structure, we are committed to establishing an unified alternative by exploring language-guided visual recognition from raw pixels. As shown in Fig. 1 (b), we aim at embedding language information into the process of visual recognition, and then directly output the language-dependent visual features. This motivation is inspired by the human cognitive mechanism towards multi-modal tasks. Neuroscience researches [5, 59, 72, 74] show that *primary visual cortex cells* can be influenced by other modalities, *e.g.*, text or sound, and then produce multimodal sensory. It means that low-level visual recognition can also be driven by natural language signals. For example, after receiving a natural language instruction, people will perform the visual recognition related to the instruction, *e.g.*, paying attention to relevant regions and analyzing information like colors or textures.

To achieve this target, we first propose a novel *Language-Guided Dynamic Convolution* (LaConv) module, of which structure is depicted

in Fig. 4. The property of “*language-guided visual recognition*” are mainly reflected in that LaConv can realize differentiated feature extractions on the same image according to different natural language instructions. This property is attributed to its dynamic convolution filters predicted by natural language information. Through this novel multi-modal convolution, LaConv can complete visual recognition and multi-modal reasoning in one processing step.

Based on LaConv, We build a fully language-guided convolution network, termed *LaConvNet*. As shown in Fig.1, LaConvNet processes the input image from the pixel level and embeds the natural language information into the whole process of visual feature learning. The output visual features can be directly used for multi-modal prediction. Such a property makes it highly generalizable to different VL tasks. For example, we can simply add a detection layer after LaConvNet for REC task. Compared to previous multi-modal networks, LaConvNet gets rid of large image backbones and unifies feature extraction and multi-modal inference in one forward structure.

To validate our approach, we first conduct experiments on four referring expression comprehension (REC) benchmark datasets, *i.e.*, RefCOCO [61], RefCOCO+ [61], RefCOCOg [56], Referit [36] and Flickr30k [65]. After pre-training on a certain amount of data, *e.g.*, Visual Genome [41], LaConvNet is comparable to a set of state-of-the-art (SOTA) methods [9, 54, 87] and large-scale pre-training models [7, 91], while maintaining superior compactness and efficiency. In addition, we validate its generalization ability on two visual reasoning datasets, *i.e.*, CLEVR [34] and CLEVR-Ref+ [48], where competitive performance can be also witnessed.

In summary, our contributions are three-fold:

- We proposed an efficient language-guided dynamic convolution block, namely *LaConv*, which can simultaneously accomplish visual feature learning and multi-modal inference.
- Based on LaConv, we proposed LaConvNet, a compact, efficient and highly generalized network for language-guided visual recognition.

- On multiple benchmarks, LaConvNet is on par with or even better than existing modular methods, while retraining superior model compactness and efficiency.

## 2 Related Work

### 2.1 Referring Expression Comprehension and Segmentation

Referring expression comprehension (REC) and Segmentation (RES) [36, 56, 65] are two popular tasks in vision-and-language research, which aim to locate the target object according to a given natural language expression. In particular, REC and RES locate the referent by bounding box and object mask, respectively. Early REC and RES works [47, 50, 92, 93] usually follow the two-stage pipeline. They typically use Faster-RCNN [69] to extract visual representations of salient objects, and then compare them to the language features to select the best-matching one. Due to the multi-step setup, these approaches are often inferior in their inference speed and performance. To this end, recent researchers have turned their attention to one-stage modeling [9, 11, 26, 32, 53, 54, 76, 77, 86–88, 98]. Specifically, these approaches first use convolution neural networks like ResNet [18] or DarkNet [68] as the visual backbone, based on which a multi-modal branch is deployed for cross-modal interactions. Then, a detection or segmentation head is used to directly output the prediction of the referent. Inspired by the great success of Transformer [79], recent advances focus on applying Transformer in REC [9, 55, 99], and RES [11, 38, 88, 89] to improve the detection ability and the reasoning ability.

Despite of the effectiveness, most approaches still rely on heavy visual backbones and expensive multi-modal fusion blocks. By contrast, LaConvNets simplify this pipeline with language-guided visual recognition, making them much more efficient than existing REC and RES approaches.

### 2.2 Visual Reasoning

Visual reasoning is an important research direction in vision and language study, which aims to examine the compositional, relational and structural reasoning abilities of multi-modal models.

Existing visual reasoning methods can be categorized into two groups: the neural-based [29, 64, 71, 85] and the symbol-based approaches [2, 22, 24, 35, 57, 58, 90], respectively. In particular, neural-based approaches [29, 64, 71, 85] aim to reason over the image based on the language instructions via attention [29, 85], relational network [71] or modulated network [64, 71]. Despite of the effectiveness, they are often inferior in their interpretability and training efficiency. In this case, some works [2, 22, 24, 35, 57, 58, 90] explore symbol-based networks to decompose visual reasoning into several pre-defined programs. These models usually learn a symbolic predictor to parse the language instructions into specific programs, and then execute the corresponding modules to predict the final answer. This methodology can ensure the interpretability and efficiency of reasoning process, but the models still heavily rely on expert knowledge in program design and require additional program annotations.

Compared to these approaches, LaConvNet mainly differs in its unified multi-modal structure, which can simultaneously perform visual recognition and multi-modal reasoning from raw pixels. Such a structure make LaConvNet more compact and efficient than existing approaches while still maintaining strong reasoning capabilities. In addition, we also show that as a neural-based approach, LaConvNet is still interpretable.

### 2.3 Language-guided Convolutions

Applying convolution to process vision and language data is not new in literature. In early attempts, convolution is used as a cross-modal module to jointly process image and text features [8, 16, 62, 64]. In terms of language-driven convolution, there are several recent methods related to our work. Specifically, FiLM [64] aims to learn normalization weights by language features and applies them after convolutions. With this design, FiLM can extract language-related visual features and achieve multi-modal reasoning. Gao *et al.* [16] propose a question-guided hybrid convolution (QGHC) module, of which the convolution kernels are also predicted by the text features. However, these dynamic kernels are independent of images and may not adapt well to different visual content. Qiu *et al.* [67] propose language-aware deformable convolution to

learn fine-grained multi-modal representation. In [67], the offsets of the deformable convolution are predicted by multi-modal features. Compared to these approaches, LaConv can generate different language-driven convolution kernels for different visual areas, therefore achieving better vision-and-language alignments. In addition, all existing multi-modal convolutions are used as plug-in components for existing modular networks. In this paper, we use the propose LaConv as a stand alone building block for fully language driven convolution network. In practice, using previous convolution modules to build the unified network are also inferior to LaConv.

## 2.4 Efficient and Unified Multi-modal Network

Recently, the design of unified multi-modal networks has gained gradually increasing interest in Vision-Language (VL) community [7, 15, 39, 43, 82]. However, most existing multi-modal models [7, 15, 43] still adopt the highly redundant architecture, which consists of a large visual backbone and deep multi-modal fusion branches. This computational expensive architecture greatly increases the costs of deployment. To improve the efficiency, some works [39, 82] handle visual processing and multi-modal fusion into a single unified manner. Among them, the most representative work is ViLT [39] which directly feeds image and text embedding into a vision transformer [12] to obtain joint vision-and-language representations. After pre-training on millions of image-text pairs, ViLT can be applied to various VL tasks, *e.g.*, VQA. Recently, Wang et.al [82] propose a ViT-like model, which is pre-trained with a novel pre-training objective, *i.e.*, prefix language modeling. Compared to ViLT, it further insert more convolution blocks at the beginning of the network.

Recently, there are also several methods [21, 52] proposed to explore the unified learning of various VL tasks. However, these methods focus more on the multi-task learning by using one multi-modal network, and their network structures are still modular and still requires large visual backbones. In this case, the contributions of these works are orthogonal to this paper.

Despite of the great success, these Transformer based models are still over-parameterized

and computationally expensive. In this case, we explore an extremely compact unified multi-modal network called LaConvNet. Due to the efficient design of language-guided dynamic convolution, LaConvNet can be much more efficient than existing unified multi-modal models.

## 3 Language-guided Dynamic Convolution

In this section, we give the definition of the proposed Language-guided Dynamic Convolution (LaConv), of which structure is illustrated in Fig.1. We first introduce its main principle of language-guided dynamic convolution, and then describe how its convolution kernels are generated from text features.

### 3.1 Definition.

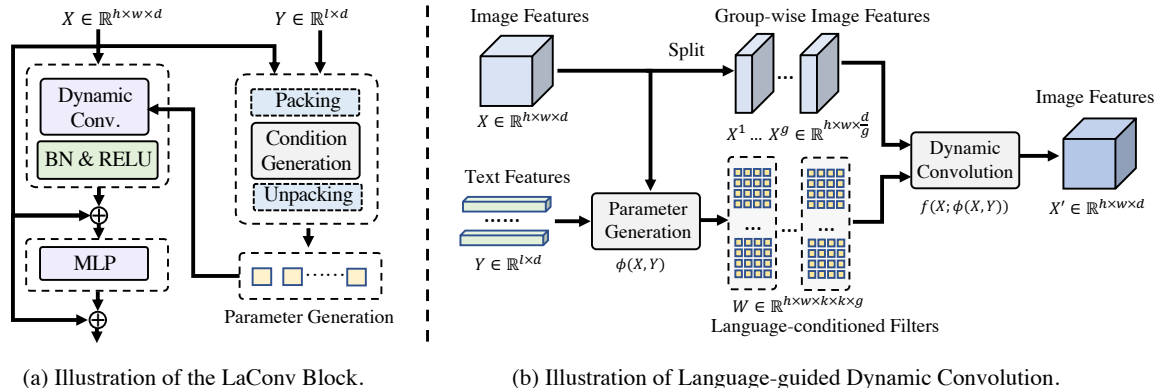
To achieve language-guided visual recognition, we propose a LaConv module in this paper. Compared to existing multi-modal modules, such as self-attention [10, 11, 89], the main difference of LaConv is that it can produce language-conditioned dynamic kernels for depth-wise convolution, thereby achieving differentiated visual feature learning for different input texts.

Specifically, given the image features  $X \in \mathbb{R}^{h \times w \times d}$  and the text features  $Y \in \mathbb{R}^{l \times d}$ , LaConv is defined by

$$X' = f(X; \phi(X, Y; \theta)). \quad (1)$$

Here,  $f(\cdot)$  denotes the convolution operation,  $\phi: X, Y \rightarrow W$  is the function of parameter generation based on image and text features, and  $\theta$  denotes the learnable parameters. Compared with common convolutions [18], of which kernels are static for all images, LaConv can produce dynamic convolution kernels based on the input text, thereby achieving language-guided visual recognition.

To improve the efficiency of LaConv,  $f(\cdot)$  and  $\phi(\cdot)$  are designed as an efficient operator and a lightweight parametric function, respectively. Specifically, we define  $f(\cdot)$  as a dynamic depth-wise convolution. Given the language-conditioned convolution kernel  $W \in \mathbb{R}^{h \times w \times k \times k \times g}$ ,  $f(\cdot)$  can be formulated by



(a) Illustration of the LaConv Block.

(b) Illustration of Language-guided Dynamic Convolution.

**Fig. 2** Illustration of the LaConv block and its language-guided dynamic convolution. (a). In LaConv block, the spatial-wise convolution kernels are generated by the language conditions, which are then used to dynamically process the visual features. (b). The parameter generation module firstly produces language-conditioned convolution filters based on image and text features. After that, language-guided dynamic convolution is conducted to process the image features.

$$\text{dyconv}(X^l)_{i,j} = \sum_{\Delta i=1}^k \sum_{\Delta j=1}^k X^l_{i+\Delta i, j+\Delta j} \odot W_{i,j,\Delta i,\Delta j,l},$$

$$f(X; W) = [\text{dyconv}(X^1), \dots, \text{dyconv}(X^g)]. \quad (2)$$

Here,  $k$  and  $g$  are the kernel size and the number of groups.  $[\cdot]$  denotes the concatenation. In practice, LaConv is much more efficient than common convolutions. Specifically, the FLOPs of  $f(\cdot)$  are  $\frac{1}{d}$  of common convolutions, where  $d$  is usually up to hundreds. Notably, although the language-conditioned convolution kernel  $W$  has a large shape, it can be predicted via  $\phi(\cdot)$  with lightweight parameters. We discuss the parameter generation in next section.

From Eq. 2, we can also observe two key differences of LaConv from the existing depth-wise convolution [42]. Firstly, in LaConv, each image position  $(i, j)$  has their corresponding filters, which is to model the spatial relationships in text information, *e.g.*, “left person”. When filters are shared, such information is hard to recognize. Secondly, with the language-conditioned convolution filters  $W$ , LaConv can extract differentiated visual features based on different texts.

LaConv also has a distinct design principle different from existing multi-modal modules [9, 11, 53, 88] that mainly apply self-attention for cross-modal interaction. The applied dynamic convolution can help LaConv achieve better visual feature learning, and the used language-conditioned

parameter generation can also facilitate the cross-modal interactions for various VL tasks. Meanwhile, its computation efficiency is also superior than the attention-based modules.

### 3.2 Language-conditioned Parameter Generation

From the definition of LaConv, the key to realize language-guided convolution lies in the design of the function of parameter generation, *i.e.*,  $\phi(\cdot)$ . As shown in Fig. 3,  $\phi(\cdot)$  needs to generate dynamic convolution filters based on natural language information. These filters are spatially and semantically related to the image. In this case, the processing of LaConv can be dynamically adjusted based on the changes of visual content and text information.

Generally, the length of the text features is often not consistent with the resolution of the image features, and they are also not spatially aligned. To this end, we first transform the text features into a condition matrix  $C \in \mathbb{R}^{(h \times w) \times d}$ , which has the same shape as the image ones. Each condition vector of  $C$  is also semantically related to the corresponding image region. In this case, the parameter generation function  $\phi(\cdot)$  can be defined by

$$\phi(X, Y; \theta) = CW_1 + b_1, \quad (3)$$

where  $C = \sigma(A(YW_A)W_C)$ .

Here,  $W_1 \in \mathbb{R}^{d \times (k \times k \times g)}$  and  $b_1 \in \mathbb{R}^{(k \times k \times g)}$  are the projection weight and bias term for predicting convolution kernels.  $W_A \in \mathbb{R}^{d \times d}$  and  $W_C \in$



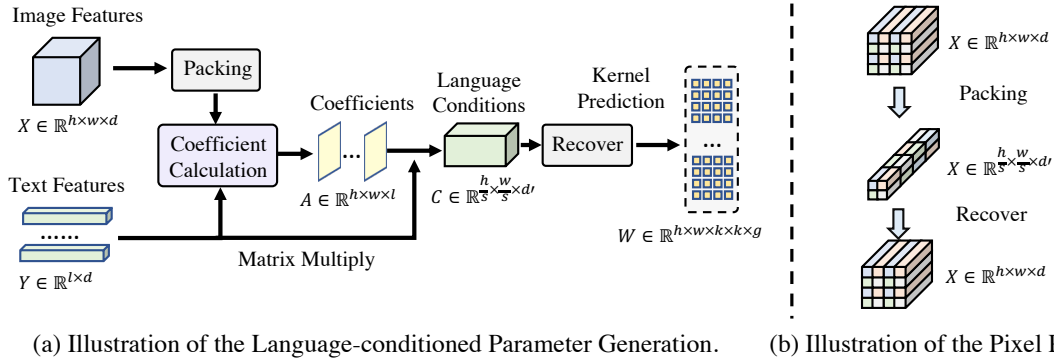


**Fig. 3** Illustration of the parameter generation and pixel packing. The input text features are first transformed into a language condition matrix, which is spatially and semantically related to the image features. Then, the convolution filters are predicted based on this condition matrix. *Pixel packing* operations are applied to alleviate the *low-rank degeneration* in low-level visual features.

$\mathbb{R}^{d \times d}$  are two projection weights for the generation of condition matrix.  $A \in \mathbb{R}^{(h \times w) \times l}$  is the affinity matrix between  $X$  and  $Y$ , and its values denotes the coefficients between the features of two modalities. Here, we resort to *scaled dot-product attention* [79] to compute the multi-modal coefficients:

$$A = \text{Softmax}\left(\frac{(XW_X)^T(YW_Y)}{\sqrt{d}}\right), \quad (4)$$

where  $W_X \in \mathbb{R}^{d \times d}$  and  $W_Y \in \mathbb{R}^{d \times d}$  are two projection weights. To improve module capacity, we also extend Eq. 4 into a *multi-head* version [79]. The mechanism of multi-modal coefficient generation is related to self-attention [79], but we only conduct attentions between two modalities, which is practically computational friendly.

With Eq.3 and Eq.4, the obtained condition matrix not only has the same shape as the visual features, but also spatially relates to the image regions. Therefore, through the condition matrix, we can effectively embed language information into dynamic parameter generations for each visual region and multi-modal example. Meanwhile, our parameter generation is actually more parameter-efficient than conventional convolutions, and its parameters are about  $\frac{3}{k^2}$  of the common convolution layer.

**Pixel packing.** Since the generation of condition matrix is based on the scale-dot product between two types of features, it is prone to the issue of *low-rank degeneration* [4] when the number of the image features is much larger than their feature dimension, *e.g.*, the low-level image features.

To this end, we introduce a tensor operation called *pixel packing* to alleviate this problem. As shown in Fig 3, given the image features  $\mathbf{I} \in \mathbb{R}^{(h \times w) \times d}$ , we first pack them into  $k$  new visual tokens, where  $k = (h \times w)/s^2$ , and each token is the concatenation of the  $s \times s$  local features. So, the number of new image features is reduced by  $s^2$  times. Correspondingly, the resolutions of the condition matrix  $C$  and the affinity matrix  $A$  in Eq. 3 also becomes  $(h \times w)/s^2$ . Before the parameter predictions, we will recover the condition matrix back to the size of  $(h \times w)$ , which is to make the predicted filters to adapt the input image features.

Overall, pixel packing is a packing-and-recover processing, which can alleviate the issue of low-rank degeneration via reducing the feature resolutions, while maintaining the multi-modal interactions. In this case, its mechanism and effect are still different to other tensor operations like patch embedding [12].

## 4 LaConvNet

Based on LaConv, we further propose a unified and end-to-end network, termed *LaConvNet*, as shown in Fig. 4. LaConvNet processes images directly from the pixel level, completely abandoning the traditional convolution backbones like ResNet [18] or MaskRCNN [19]. This property is the main difference between LaConvNet and most existing VL systems, which also makes LaConvNet much more compact. Specifically, we first construct the basic LaConv block, and the  $i$ -th layer can be formulated by

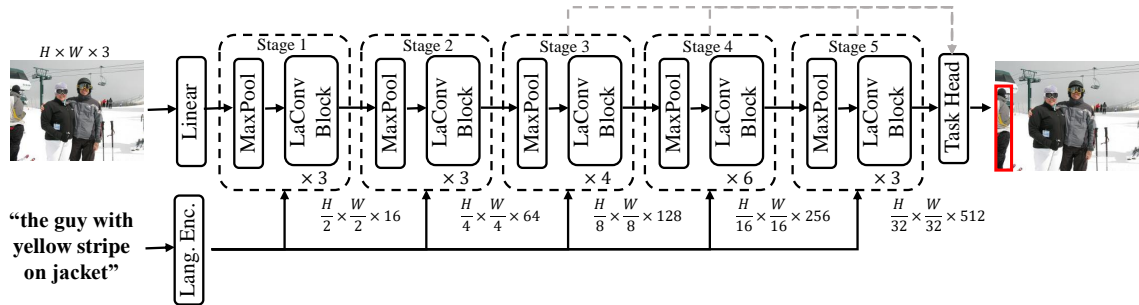


**Fig. 4** The architecture of LaConvNet. LaConvNet consists of 5 stages, each of which has a max pooling layer and several LaConv blocks. The input image and text are firstly processed by a linear projection and a language encoder, respectively. Afterwards, LaConv blocks are used to extract visual features based on language information. Finally, the task-specific head is applied to predict the results of the task.

$$\begin{aligned} X'_i &= \sigma(\text{BN}(f(X_{i-1}; \phi(X_{i-1}, Y))) + X_{i-1}), \\ X_i &= \text{MLP}(X'_i) + X'_i, \end{aligned} \quad (5)$$

where  $\sigma$  denote the activation function and BN is the batch normalization layer. In Eq. 5, the MLP layer is formulated by

$$\text{MLP}(X) = \text{BN}(\sigma(\text{BN}(XW_a))W_b), \quad (6)$$

where  $W_a \in \mathbb{R}^{d \times 4d}$  and  $W_b \in \mathbb{R}^{4d \times d}$  are two projection weights.

Based on the LaConv block, we propose two versions of LaConvNet, termed *LaConvNet-S* and *LaConvNet-B*. LaConvNet-S and LaConvNet-B contain 10 and 19 LaConv blocks, respectively. For each stage of LaConvNet, we set a proper *packing size*  $s$  to keep the expressive power of the parameter generation. The detailed configurations are shown in Tab. 1.

Notably, the design of LaConvNet still has a large space for exploration, such as the choice of depth, width, filter size *etc.* In this paper, we only aim to provide an effective baseline network to quickly validate our motivation.

## 5 Experiments

To validate LaConvNet and the LaConv module, we conduct extensive experiments on four benchmark datasets of Referring Expression Comprehension (REC) and Segmentation (RES) and Visual Question Answering (VQA), namely RefCOCO [36], RefCOCO+ [36], RefCOCOg [56], Referit [36], Flickr30k Entities [65], CLEVR [34]

and CLEVR-Ref+ [48], and compare them with a set of latest methods [29, 37, 54, 73, 87].

### 5.1 Datasets and Metrics

**RefCOCO** [36], **RefCOCO+** [36] and **RefCOCOg** [56] are three datasets for referring expression comprehension and segmentation, which are collected via an interactive game interface. RefCOCO and RefCOCO+ are splitted into *train*, *val*, *test A* and *test B*. The referents of *test A* are about people, while the ones of *test B* are objects. In contrast, RefCOCOg contains a *val* and a *test*. In RefCOCO and RefCOCO+, there are 142k expressions for 50k bounding boxes of 20k images from MS-COCO [44]. The expressions of RefCOCO are mainly about absolute locations, while the ones of RefCOCO+ are more about relative relations. RefCOCOg has 104k expressions for 54k bounding boxes from 26k images. The expressions of RefCOCOg are longer and more complex.

Following previous works [54, 86, 88], IoU and IoU@0.5 are used to measure the performance of REC and RES tasks, respectively. In particular, IoU determines the the Intersection-over-Union (**IoU**) between the prediction and ground-truth. For IoU@0.5, when the IoU score is large than 0.5, the prediction is regarded as correct.

**Referit** [36] includes 20,000 images from SAIAPR-12 dataset [13]. In Referit, there are 54,127, 5,872 and 60,103 image-expression pairs in the training, validation and testing sets, respectively. Compared to RefCOCO, RefCOCO+ and RefCOCOg, Referit contains more descriptions about the background. We use IoU@0.5 as the metric for REC task.

**Table 1** Network architecture of LaConvNet. “ $n - d$ ” denotes the channels of transformations. “s” denotes the packing size of the LaConv block. Similar to ResNet, LaConvNet contains 5 stages and each stage has several LaConv blocks.

Output Size	s	LaConvNet-S	LaConvNet-B
$224 \times 224$	-	16-d linear	16-d linear
$112 \times 112$	-	2x2, stride 2 pool	2x2, stride 2 pool
$112 \times 112$	8	3x3, 16-d LaConv $\times$ 2	3x3, 16-d LaConv $\times$ 3
$56 \times 56$	-	2x2, stride 2 pool	2x2, stride 2 pool
$56 \times 56$	4	7x7, 64-d LaConv $\times$ 1	7x7, 64-d LaConv $\times$ 3
$28 \times 28$	-	2x2, stride 2 pool	2x2, stride 2 pool
$28 \times 28$	2	7x7, 128-d LaConv $\times$ 2	7x7, 128-d LaConv $\times$ 4
$14 \times 14$	-	2x2, stride 2 pool	2x2, stride 2 pool
$14 \times 14$	1	7x7, 256-d LaConv $\times$ 4	7x7, 256-d LaConv $\times$ 6
$7 \times 7$	-	2x2, stride 2 pool	2x2, stride 2 pool
$7 \times 7$	1	7x7, 512-d LaConv $\times$ 1	7x7, 512-d LaConv $\times$ 3
Classifier			

**GRefCOCO** [46] is a large scale dataset for generalized referring expression comprehension. It includes 90,022 multi-target expressions and 32,202 no-target expressions for 19,994 images in the *train*, *val*, *testA* and *testB* splits. Since the *testA* and *testB* splits are not released, we report T-acc [46], N-acc [46], cIoU [46] and gIoU [46] on *val* set.

**Flickr30k Entities** [65] contains about 427,000 expressions for 31,7183 images, 29,783 images are used for training, 1000 for validation, and 1000 for testing. Compared to other REC datasets, the expressions of Flickr30k may refer to multiple objects. Following the common settings [9, 86], we merge all boxes of referred objects into a single one. IoU@0.5 is used as the metric.

**CLEVR** [34] is a synthetic VQA dataset introduced by Johnson *et al* [34], which aims to examine various reasoning skills, *e.g.*, relation and counting. It contains 999k image-question pairs, where 700k, 150k and 150k examples are for training, validation and test, respectively. We use the classification accuracy as the metric.

**CLEVR-Ref+** [48] is a synthetic RES dataset derived from CLEVR. It aims to examine referring expression comprehension with a set of reasoning tasks under the settings of one or multiple referents. CLEVR-Ref+ contains 70K images

and 700k expressions. We use the overall IoU to measure the accuracy.

## 5.2 Experimental Settings

**LaConvNet.** We use Glove [63] word embeddings with a dimension of 300 to represent each input word. The language encoder is built with an LSTM network and a self-attention layer [79], and their dimension are set to 512. The input images are resized to  $416 \times 416$ ,  $320 \times 320$  and  $224 \times 224$  for REC, RES and VQA, respectively. The task-specific heads of LaConvNet are directly borrowed from previous works [54, 94]. For REC, the output three-scale visual features are firstly fused by a simple multi-scale fusion module [54], upon which a detection head [68] is used to predict the target box. For VQA, we first attentively pool the last-layer visual features and the language features and then fuse them by additions, followed by an MLP to predict the answer.

All models are trained by *Adam* optimizer [40] with an initial learning rate of 1e-4. For REC task, the total training epochs are set to 25, 3 of which are for warm-up, and the learning rate is decayed by cosine schedule. We pre-train LaConvNets on VG+COCO+Flickr (200k images) with 10 epochs. For CLEVR and CLEVR-ref+, the number of



**Table 2** Comparisons of LaConvNet and existing REC models on RefCOCO, RefCOCO+ and RefCOCOg. #Params denotes the parameter size. \* denotes the reproduced results. “cls-token” and “det-head” denotes that the prediction head of TransVG and LaConvNet, respectively.

Models	#Params	FLOPs	RefCOCO			RefCOCO+			RefCOCOg	
			val	testA	testB	val	testA	testB	val	test
<i>two-stage models:</i>										
CMN [23]	-	-	-	71.03	65.77	-	54.32	47.76	-	-
MAttNet [92]	90M	~81G	76.65	81.14	69.99	65.33	71.62	56.02	66.58	67.27
NMTree [47]	-	-	76.41	81.21	70.09	66.46	72.02	57.52	65.87	66.44
CM-Att-Erase [50]	-	-	78.35	83.14	71.32	68.09	73.65	58.03	67.99	68.67
<i>one-stage models:</i>										
RealGIN [98]	73M	28.3G	77.25	78.70	72.10	62.78	67.17	54.21	62.75	62.33
FAOA [86]	183M	17.8G	72.54	74.35	68.50	56.81	60.23	49.60	61.33	60.36
ReSC [87]	182M	57.1G	77.63	80.45	72.30	63.59	68.36	56.81	67.30	67.20
MCN [54]	73M	44.5G	80.08	82.29	74.98	67.16	72.86	57.31	66.46	66.01
LBYL-Net [26]	115M	-	79.67	82.91	74.15	68.64	73.38	59.49	-	-
TransVG [9]	168M	73.1G	81.02	82.72	78.35	64.82	70.70	56.94	68.67	67.73
<i>pre-trained models:</i>										
UNITER-L [7]	396M	961.6G	81.41	87.04	74.17	75.90	81.45	66.70	74.86	75.77
VILLA-L [15]	399M	1060.1G	<u>82.39</u>	<u>87.48</u>	<u>74.84</u>	<u>76.17</u>	<u>81.54</u>	<u>66.84</u>	<u>76.18</u>	<u>76.71</u>
ViLT [39] (cls-token)*	112M	42.0G	79.51	82.15	71.93	65.32	71.30	54.63	67.03	66.35
ViLT [39] (det-head)*	111M	42.0G	79.11	81.90	73.21	68.16	73.35	57.35	67.16	66.47
LaConvNet-S	24M	8.9G	80.26	83.51	75.82	69.82	73.61	60.98	74.45	74.54
LaConvNet-B	35M	14.5G	<b>82.46</b>	84.66	<b>78.16</b>	72.31	76.57	63.76	<b>76.37</b>	<b>76.75</b>

**Table 3** Comparison of LaConvNet and existing REC models on Referit and Flickr. \* denotes the reproduced results.

Models	#Params	FLOPs	Referit	Flickr
			test	test
<i>two-stage models:</i>				
MAttNet [92]	90M	~81G	29.04	-
SimNet [80]	-	-	34.54	60.89
DDPN [93]	-	-	63.00	73.30
<i>one-stage models:</i>				
ZSGNet [70]	-	-	58.63	63.39
FAOA [86]	183M	17.8G	60.67	68.71
ReSC [87]	182M	57.1G	64.60	69.28
TransVG [9]	168M	73.1G	<u>70.73</u>	<u>79.10</u>
LaConvNet-S	24M	8.9G	72.02	77.87
LaConvNet-B	35M	14.5G	<b>74.28</b>	<b>79.95</b>

training epochs is 23, and 3 epochs are for warm-up, and the learning rate is decayed by a factor of 0.2 at the 20-th and the 22-th epochs. For CLEVR

and CLEVR-ref+, LaConvNets are trained from scratch.

**ViLT [39]**. To adopt ViLT to REC task, we try two types of REC heads [9, 54] on ViLT. In the first setting, we use a 4-layer MLP to predict the box based on the [CLS] token [9]. In the other setting, ViLT predicts the box through an anchor-based detection head [68]. Fine-tuning ViLT takes 60 epochs with a learning rate of 1e-4. We use AdamW as the optimizer. Following [9], we apply some data augmentations to avoid overfitting.

## 5.3 Experimental Results

### 5.3.1 Quantitative Analysis

**Referring Expression Comprehension (REC)**. In Tab. 2 - 3, we compare LaConvNets with existing REC models on five common REC benchmark datasets *i.e.*, RefCOCO, RefCOCO+, RefCOCOg, ReferIt and Flickr30K. The first observation from these tables is that LaConvNet-S can already outperform existing one-stage and

**Table 4** Comparison with the State-of-the-art methods on three RES datasets. The results colored in gray means that their visual backbone is much large than LaConvNet. \* denotes the reproduced results. † denotes that large pre-trained language model is used as the text encoder.

Models	#Params	FLOPs	Visual Backbone	RefCOCO			RefCOCO+			RefCOCOg	
				val	testA	testB	val	testA	testB	val	test
MAttNet [92]	90M	~81G	MRCNN	56.51	62.37	51.70	46.67	52.39	40.08	47.64	48.61
CMSA [89]	-	-	DR101	58.32	60.61	55.09	43.76	47.60	37.89	-	-
STEP [6]	-	-	DR101	60.04	63.46	57.97	48.19	52.33	40.41	-	-
BRINet [25]	241M	367.6G	DR101	60.98	62.99	59.21	48.17	52.32	42.11	-	-
CMPC [27]	118M	126.6G	DR101	61.36	64.53	59.64	49.56	53.44	43.23	-	-
LSCM [31]	128M	130.4G	DR101	61.47	64.99	59.55	49.34	53.12	43.50	-	-
CMPC+ [49]	-	-	DR101	62.47	65.08	60.82	50.25	54.04	43.47	-	-
MCN [54]	73M	44.5G	DN53	62.44	64.20	59.71	50.62	54.99	44.69	49.22	49.40
EFN [14]	232M	124.7G	R101	62.76	65.69	59.67	51.50	55.24	43.01	-	-
BUSNet [84]	-	-	DR101	63.27	66.41	61.39	51.76	56.87	44.13	-	-
CGAN [53]	70M	51.7G	DR101	64.86	68.04	62.07	51.03	55.51	44.06	51.01	51.69
LTS [33]	-	-	DN53	65.43	67.76	63.08	54.21	58.32	48.02	54.40	54.25
VLT [10, 11]	89M	142.5G	DN53	67.52	70.47	65.24	56.30	60.98	50.08	54.96	57.73
LAVT [88]†*	46M	87.8G	Swin-T	<u>69.27</u>	<u>72.16</u>	<u>65.59</u>	<u>57.02</u>	<u>62.52</u>	<u>49.26</u>	<u>58.76</u>	<u>60.14</u>
ReSTR [38]	122M	52.3G	ViT-B	67.22	69.30	64.45	55.78	60.44	48.27	-	-
LAVT [88]†	118M	193.1G	Swin-B	72.73	75.82	68.79	62.14	68.38	55.10	61.24	62.09
VLT [11]†	-	-	Swin-B	72.96	75.96	69.60	63.53	68.43	56.92	63.49	66.22
LaConvNet-S	24M	9.6G	None	69.74	72.21	67.29	57.16	60.11	47.72	60.89	60.48
LaConvNet-B	35M	15.7G	None	<b>70.59</b>	<b>72.93</b>	<b>67.74</b>	<b>60.43</b>	<b>64.47</b>	<b>52.02</b>	<b>61.73</b>	<b>62.41</b>

**Table 5** Comparisons of LaConvNet with existing approaches on Clevr-Ref+ dataset. *Prog* denotes the number of extra program labels used during training. Since the FLOPs of IEP-Ref vary dynamically for different samples, we report the average FLOPs of 100 samples.

Models	#Params	FLOPs	Prog	IoU
RMI [45]	-	-	0	56.1
IEP-Ref [48]	49M	~11.2G	9K	76.0
IEP-Ref [48]	49M	~11.2G	18K	78.2
IEP-Ref [48]	49M	~11.2G	700K	80.6
IEP-Ref [48]	49M	~11.2G	GT	<u>81.6</u>
LaConvNet-S	23M	5.3G	0	79.8
LaConvNet-B	35M	8.6G	0	<b>82.3</b>

two-stage approaches by notable margins, *e.g.*, +5.78% over TransVG [9] and +6.46% over CM-Att-Erase [50]. To explain, visual features of these modular networks are usually redundant and noisy [20], and inevitably hurt the efficiency of multi-modal reasoning. By contrast, LaConvNets directly extract language-relevant visual features from raw pixels, greatly improving the quality and compactness of visual features. As the model size

**Table 6** Results of LaConvNet and existing methods on gRefCOCO *val* set. Following the settings of RLA [46], output masks with less than 50 positive pixels are regarded as non-target predictions. † denotes that no-target classifier is applied.

Models	cIoU	gIoU	N-acc	T-acc
MAttNet [92]	47.51	48.24	41.15	96.13
LTS [33]	52.30	52.70	-	-
VLT [11]	52.51	52.00	47.17	95.72
CRIS [81]	55.34	56.27	-	-
LAVT [88]	57.64	58.40	49.32	96.18
RLA [46]	-	-	49.96	96.28
RLA [46]†	<u>62.42</u>	<u>63.60</u>	<u>56.37</u>	<u>96.32</u>
LaConvNet-S	57.06	<b>62.83</b>	<b>59.16</b>	99.65
LaConvNet-B	<b>57.14</b>	62.52	58.06	<b>99.74</b>

increases, LaConvNet-B can obtain obvious performance gains, suggesting its superior scalability. Notably, the performance gains of LaConvNets are more obvious on more challenging dataset, *i.e.*, RefCOCOg, confirming its superior ability in visual reasoning. On ReferIt and Flickr, whose data distributions are greatly different from the RefCOCO-series, LaConvNets can also

**Table 7** Comparisons of LaConvNet and existing methods on CLEVR. #Params denotes the parameter size. \* denotes the reproduced results.

Model	#Params	FLOPs	Overall Accuracy	Count	Cmp. Num.	Exist	Query. Attr.	Cmp. Attr.
BUTD [1]*	66M	8.9G	50.6	44.2	68.7	64.3	44.5	53.7
Film [64]	-	-	97.6	94.5	93.8	99.2	99.2	99.0
RN [71]	-	-	95.5	90.1	93.6	97.8	97.1	97.1
BAN [37]*	147M	19.1G	92.2	88.3	94.9	96.4	91.2	94.7
RAMEN [73]*	76M	8.1G	87.8	82.1	83.3	93.9	90.6	87.0
DDprog [75]	-	-	98.3	96.5	98.4	98.8	99.1	99.0
Tbdnet [58]	-	-	98.7	96.8	99.1	98.9	99.4	99.2
NS-CL [57]	-	-	98.9	<b>98.2</b>	99.0	98.8	99.3	99.1
MACNet [29]	39M	8.0G	<u>98.9</u>	97.1	<u>99.1</u>	<u>99.5</u>	<u>99.5</u>	<b>99.5</b>
LaConvNet-S	19M	1.9G	98.3	96.4	97.5	99.2	99.3	98.3
LaConvNet-B	31M	3.7G	<b>99.1</b>	97.9	<b>99.4</b>	<b>99.5</b>	<b>99.6</b>	99.3

**Table 8** Comparison of LaConvNets and other multi-task VL models on VQAv2 and SNLI-VE. UniT is a VL transformer that can simultaneously learn different tasks. We report accuracy on *test-dev* set of VQAv2 and *test* set of SNLI-VE.

Methods	#Params	VQAv2	SNLI-VE
Unified-IO <sub>base</sub> [52]	241M	61.8	-
UniT-single-task [21]	201M	66.38	70.52
UniT-shared [21]	201M	66.97	73.16
LaConvNet-S	~25M	66.58	71.77
LaConvNet-B	~36M	<b>67.21</b>	74.21

outperform existing REC models with significant improvements. In addition to performance, we can also see the superiorities of LaConvNets in parameter size and model efficiency. In particular, the total parameters of LaConvNet-S are 1/7 of TransVG. In terms of FLOPs, the total cost of LaConvNet-S is even 262 times cheaper than the one of TransVG. Compared to other one-stage REC models, the same advantages can be still witnessed, confirming the great potential of LaConvNets on edge devices.

In Tab. 2, we also compare LaConvNets with large-scale pre-trained models, *i.e.*, UNITER [7], VILLA [15] and ViLT [39]. All these large-scale models require about 4M images for pre-training. By contrast, LaConvNets use much fewer pre-training data, *i.e.*, 200k images, but their performance is still comparable with those large-scale pre-trained models, *e.g.*, +0.19% gains over

VILLA-L on RefCOCOg. Compared to the existing unified model ViLT, which is also pre-trained on large-scale data, LaConvNets not only performs better than ViLT, but also have much cheaper computational costs than ViLT, *i.e.*, 8.9G FLOPs *vs.* 42.0G FLOPs.

Overall, these results reveal that LaConvNet, as a multi-modal and end-to-end network, is capable of accurate vision-and-language alignments. It also confirms that LaConvNet can be a viable alternative to existing modular networks.

### Referring Expression Segmentation (RES).

In Tab. 4 and 7, we compare LaConvNets with existing RES models on RefCOCO, RefCOCO+, RefCOCOg and CLEVR-ref+. In Tab. 4, our experiments show that existing RES models incur high computational costs. For instance, VLT achieves state-of-the-art performance but requires a computational overhead of 142.5G FLOPs. LAVT [88] directly embeds language information into visual backbone, but its computational cost remains expensive due to its large visual backbone and heavy multi-modal fusion blocks. In particular, when LAVT uses Swin-B [51] as the visual backbone, its FLOPs can be up to 193.1G FLOPs. Even using the smallest size of Swin Transformer as the visual backbone, *i.e.*, Swin-T [51], the parameters and computation costs of LAVT also exceed those of LaConvNet-S by 2 times and 9 times, respectively. Compared to these methods, LaConvNets achieve better trade-offs between efficiency and performance under

**Table 9** Performance comparison between the modular network with LaConv and other methods on REC and VQA. *Prog.* denotes the number of extra program ground truths used during training. *LaConv*×6 is a structure with 6 LaConv layers. CDN and R101 denote the visual backbones, *i.e.*, CspDarkNet and ResNet101, respectively.

REC Task					VQA Task		
Models	RefCOCO		RefCOCO+		Models	Prog.	CLEVR Accuracy
	testA	testB	testA	testB			
NMTree [47]	81.21	70.09	72.02	57.52	DDprog [75]	700k	98.3
CM-Att-Erase [50]	<u>83.14</u>	71.32	73.65	58.03	Tbdnet [58]	700k	98.7
MCN [54]	82.29	74.98	72.86	57.31	MACNet [29]	0	<u>98.9</u>
TransVG [9]	82.72	<u>78.35</u>	<u>70.70</u>	<u>56.94</u>	NS-CL [57]	0	<u>98.9</u>
LaConv×6+CDN	<b>86.02</b>	<b>79.49</b>	<b>77.24</b>	<b>62.53</b>	LaConv×6+R101	0	<b>99.1</b>

**Table 10** Ablation study of dynamic filters and parameter generation in LaConv. We conduct all experiments based on LaConvNet-S. *LPG* denotes the language-conditioned parameter generations.

Settings	Params	FLOPs	RefCOCO
<i>dynamic filters:</i>			
group=1	22M	8.0G	77.02
kernel=3	22M	8.1G	77.78
kernels=[3,7,7,7,7]	24M	8.9G	80.26
<i>parameter generation:</i>			
no pixel packing	22M	9.1G	79.12
language only	19M	6.4G	75.58
LPG + pixel packing	24M	8.9G	80.26

the similar experimental settings, *e.g.*, the text encoder and the visual encoder with comparable parameter size. For instance, LaConvNet-S achieves better results than VLT (DN53) while requiring only 6.7% FLOPs and 27% parameters of VLT. As the model size increases, LaConvNet-B outperforms LAVT (Swin-T) by 2.15%, 3.41%, and 2.97% on RefCOCO, RefCOCO+, and RefCOCOg, respectively. Although LAVT (Swin-B) and VLT (Swin-B) can outperform LaConvNets with a large visual backbone and text encoder, their computational costs can be up to 20 times that of LaConvNet-S. Overall, we believe that LaConvNets can still be an efficient alternative to these large models for RES tasks.

In Tab. 5, we compare LaConvNets with other approaches on the synthetic RES dataset called Clevr-Ref+. This dataset contains longer and more complex expressions, which require higher reasoning ability. We observe that LaConvNets outperform other compared approaches with much fewer parameters and computations. Compared

to RMI, the end-to-end RES model, the performance gains of LaConvNets are significant, *i.e.*, up to +26.2% IoU. Although the symbol-based approaches, *e.g.*, IEP-Ref, use all ground-truth programs, their performances are still inferior to LaConvNet-B. These results further confirm the effectiveness and efficiency of LaConvNets.

In Tab. 6, we validate the robustness of LaConvNets on gRefCOCO [46], which contains single-object, multi-object and no-target expressions. From the results, we firstly observe that LaConvNet-S achieves 59.16% N-acc and 99.65% T-acc on gRefCOCO val set, which outperforms the state-of-the-art model, *i.e.*, RLA [46], by +2.79% and +3.33%, respectively. Such results suggest that LaConvNets can well handle no-target expressions. In terms of multi-object expressions, LaConvNets also have competitive performance. For instance, LaConvNet-S achieves 62.83% gIoU on gRefCOCO *val* set, which suppresses most existing RES models [11, 81, 88]. Overall, these results greatly confirm the robustness of LaConvNets.

**Visual Question Answering (VQA).** To validate the generalization ability of LaConvNets, we also apply LaConvNets to VQA task, of which results are given in Tab. 7 and 8. In Tab. 7, we compare LaConvNets with existing methods on CLEVR. From it we can see that LaConvNet-B achieves superior overall accuracy than existing approaches and also demonstrates better parameter efficiency. On multiple metrics, LaConvNet-B reaches the performance upper bound of the dataset, showing its strong reasoning ability.

We further compare LaConvNets with the multi-task Transformer model, *i.e.*, UniT [21],

**Table 11** Comparisons of LaConv block and other multi-modal modules. To make a fair comparison, we directly replace all LaConv blocks of LaConvNet-S with these multi-modal modules.

Modules	Params	FLOPs	RefCOCO	RefCOCO+
LaConv	23.1M	8.9G	80.26	69.82
FiLM [64]	30.4M	9.8G	78.95	68.78
QGHC [16]	55.7M	6.8G	76.26	66.11

on two real-world VQA benchmark datasets. In particular, UniT is a multi-modal and multi-task network, which can simultaneously conduct tasks of different modalities. In terms of network architecture, they are still modular and require independent visual backbones and another fusion branches. In contrast, LaConvNets jointly models vision-language information in one unified multi-modal network from raw pixel level, greatly reducing computational overhead. On VQAv2 and SNLI-VE, UniT requires 201M parameters, about 5 times that of LaConvNet-B. In term of performance, LaConvNets also achieve better results, *i.e.*, +0.24 on VQAv2 and +1.05 on SNLI-VE. These results demonstrate the high efficiency and generalization ability of LaConvNets. We believe that LaConvNets can be a good supplement to existing VL research which mainly pursue giant Transformer-based models to break the limit of VL learning ability.

### 5.3.2 Ablation Study

To gain deep insights of LaConvNets, we provide the detailed ablation results in Tab. 9-11.

**Ablations of LaConv.** In Tab. 10, we provide four different settings for the dynamic filters and parameter generation of LaConv:

- “Group=1” denotes that all convolution groups are set to 1 in LaConvNet.
- “Kernel=3” denotes kernel size of LaConv.
- “No pixel packing” denotes that we remove pixel packing in the language-conditioned parameter generation, as mentioned in Sec 3.2.
- “Language only” denotes that the convolution kernels are directly predicted by the language features. In this case, the generated convolution kernels are shared for all regions.

**Table 12** Parameters and FLOPs of LaConv and other modules. “VP” and “MF” denotes the visual processing module in visual backbone and multi-modal module in fusion branch, respectively. We calculate the costs of a single layer. For VLT, “MF” only calculates the costs of Transformer decoder.

Models	#Param			FLOPs		
	VP	MF	Total	VP	MF	Total
VLT [11]	5.2M	4.1M	9.3M	1.0G	2.96G	3.96G
LAVT [88]	12.5M	7.8M	20.3M	3.8G	1.0G	4.8G
ViLT [39]	7.0M		7.0M	2.1G		2.1G
LaConvNet	1.4M		1.4M	0.45G		0.45G

From Tab. 10, we observe that fewer convolution groups and smaller convolution kernels will hinder model performance. To explain, more convolution groups can often improve the model capacity and larger convolution kernels can increase the receptive fields. Such observations are also consistent with those of existing conventional convolution networks [78]. In Tab. 10, we also validate different settings of parameter generation. One can be seen that when pixel packing is removed, the model performance declines and the computational costs increase. Such results also validate the problem of *low-rank degeneration* [4] in parameter generations. From the results of “*language only*”, we can see the effectiveness of the condition matrix design. Without the transformation of condition matrix, the generated convolution kernels are image-irrelevant and shared for all visual regions. As it can be seen, this alternative design makes the model decline greatly in performance. It also suggests the importance of the proposed language-conditioned parameter generation.

**Comparison of different multi-modal convolutions.** In Tab. 11, we compare LaConv with other multi-modal convolutions in the architecture of LaConvNet, *i.e.*, FiLM [64] and QGHC [79]. In particular, FiLM directly fuses language information into the visual processing via language-conditioned normalization layers. This principle also closes to that of LAVT [88]. These approaches still rely on additional heavy multi-modal fusion blocks, which limit their efficiency. Compared to them, LaConv unify the multi-modal fusion and visual processing into one lightweight block, leading to better performance and efficiency, as shown in Tab. 11. QGHC [16], which also predicts convolution kernels by language features, takes fewer



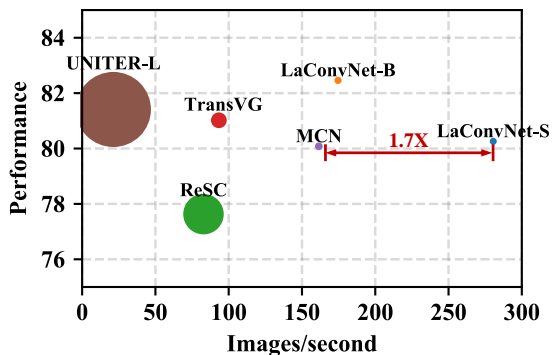


**Fig. 5** The GPU latencies and memory of LaConvNets and other models on RefCOCO. The point size corresponds to the GPU memory footprint. All models are tested on a NVIDIA A100 GPU with a mini-batch of 64.

FLOPs than LaConv, but its performance is still far behind LaConv. In summary, compared to these multi-modal modules, LaConv can achieve better trade-offs between efficiency and effectiveness.

### Results of LaConv in modular networks.

In Tab. 9, we also validate LaConv as a plug-in module to the existing modular network, of which results are given in Tab. 9. Specifically, we construct a modular network with 6 LaConv layers and a visual backbone. From this table, we can see that as a multi-modal inference module, LaConv still outperforms existing methods on REC and VQA. For example, LaConv $\times$ 6+CDN outperforms TransVG by +7.17% on RefCOCO+. On VQA, the same advantages can be also witnessed. Compared to the symbol-based approach, *i.e.*, Tbdnet [58], which uses all program ground-truth during training, LaConv still outperforms this method by +0.2% without additional program annotations. Notably, this performance almost reaches the upper-bound of CLEVR. These results demonstrate the strong generalization ability of LaConv as an plug-and-play module for VL tasks.

### 5.3.3 Model Efficiency

The efficiency of LaConvNet is depicted in Tab. 2-8 and 12, and Fig. 5. In Tab. 2-8, we compare LaConvNets with existing models in terms of parameter size and computation, *i.e.*, FLOPs. As a language-conditioned convolution network, LaConvNets are much more lightweight and efficient than existing networks, as discussed in Sec. 5.3.1.

In Tab. 12, we compare the costs of LaConv and other modules in existing methods [11, 39, 88]. By comparison, we find that existing multimodal fusion methods require much more expensive parameters and computation than LaConvNet. For example, the fusion block of VLT requires 2.96G FLOPs, about 6.5 times that of LaConvNet. Meanwhile, most existing approaches still require additional costs for the visual processing module, *e.g.*, 2.96G FLOPs of VLT, which further reduce their efficiency.

In Fig. 5, we further present the practical GPU throughputs and memory of LaConvNets. Compared to large-scale pre-trained model, *i.e.*, UNITER [7], LaConvNets are superior in both throughputs and memory costs. We also see that LaConvNet-S is more efficient than existing one-stage models, *e.g.*, 1.7 times faster than MCN [54], which is a real-time one-stage REC model. These experiments well support the efficiency of LaConvNets.

### 5.3.4 Qualitative Analysis

In this section, we give detailed visualizations to answer two key questions of LaConv and LaConvNet, *i.e.*, “*is the parameter generation reliable and interpretable?*” and “*what convolutions are learned from the natural language instructions?*” Besides, we also provide typical failure cases to further analyze LaConvNets.

**Is the condition generator reliable and interpretable?** LaConv is more interpretable than the traditional convolution due to the language-dependent parameter generation. To support this argument, we select the last convolution layer of LaConvNets to visualize the affinity matrix  $A$  in the parameter generations. As shown in Fig 6, each phrase of a text attends to the corresponding region. For instance, in the first example of Fig.6 (a), the different phrases of “a hot dog” and “on top” highlights the corresponding regions. Analogically, the spatial phrase of “the right of” in the second example of of Fig.6 (b) is also related to the *right* object. In addition, other referring phrases, *e.g.*, “the large shiny object” and “the tiny object”, are also visualized in the attention maps. Based on these observations, we believe that the generated convolution filters of a position can accurately execute the

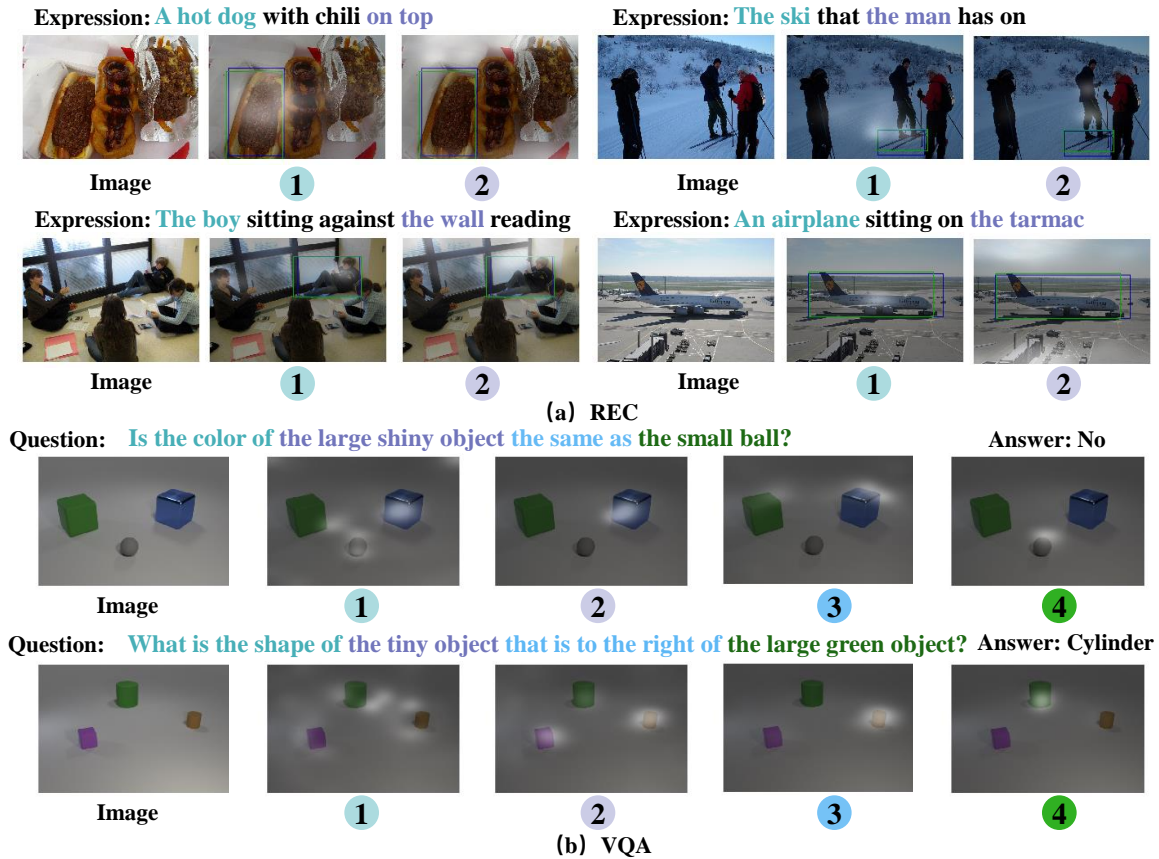


**Fig. 6** Visualizations of the attention maps in language-conditioned parameter generation. We visualize phrases of a question and their corresponding visual attention. In language-conditioned parameter generation, the phrase and its corresponding visual regions are accurately aligned.

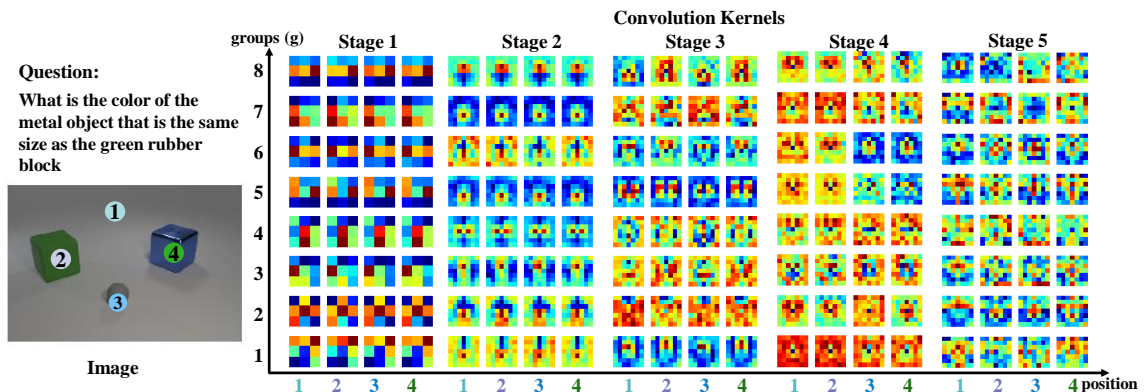


**Fig. 7** Visualizations of the dependences of text phrases and their corresponding image regions during language-conditioned parameter generation. The colors denote the magnitude of values in filters, and the redder color indicates a larger value. For each stage, we select the last layer for visualization.

corresponding language instructions, which makes LaConv more reliable and interpretable.

**What convolutions are learned from language instructions?** Unlike the conventional

convolutions that are weight-sharing for each spatial position, LaConv depends on both image position and text content. To examine its dynamics, we visualize the filters in each stage of LaConvNet

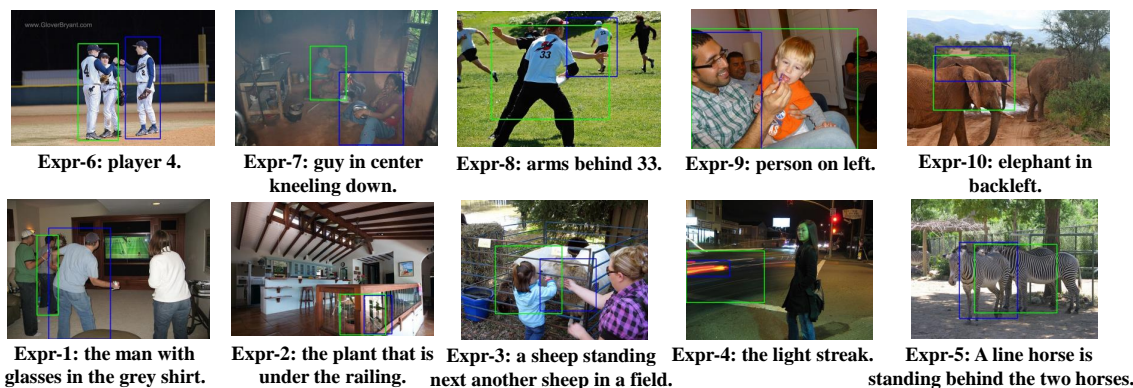


**Fig. 8** Failure cases of LaConvNet-S on RefCOCO+ (top row) and RefCOCOg (bottom row). The blue and green boxes are the ground-truths and predictions, respectively.

in Fig. 7. For a better understanding, we select four positions of the example image, and visualize their filters. From Fig. 7, the first observation is that the filters for different groups vary greatly (from the vertical axis), which suggests that each group of convolutions is responsible for different recognition patterns. The second observation is that the filters at the initial stage are relatively static, *i.e.*, filters of the same group are similar for different positions (read from the horizontal axis). Such a finding suggests that these convolutions focus on learning low-level visual representations, and they are less affected by natural language information. However, we notice that as the recognition progresses, the filters of the same group vary drastically, presenting different intensities and morphs, *e.g.*, Stage3-5. This observations suggest that the language instructions start to dynamically guide the visual recognition, so different positions present distinct patterns. Conclusively, these visualizations indicate that the language-guided visual recognition of LaConvNet is a continuous process, and the impact of language information can be reflected on its weights.

**Failure cases.** In Fig. 8, we give the typical failure cases on REC. We observe that some failure examples occur due to the ambiguous annotations, *e.g.*, Expr-2, Expr-6 and Expr-9. Meanwhile, visual occlusion is also a main factor for incorrect recognition, *e.g.*, Expr-5, Expr-8 and Expr-10. In addition, we also find that LaConvNets fail to accomplish very abstract descriptions, *e.g.*, “player 4” and “arms behind 33”. However, these types of examples are not common in existing datasets. And they has gone beyond the scope of the conventional REC research.

## 6 Conclusion

In this paper, we establish the first fully language-driven convolution network for vision-and-language tasks, termed LaConvNet, which can get rid of large visual backbones and achieve language-guided visual recognition. Specifically, LaConvNet is built by a novel dynamic convolution module called LaConv. The convolution kernels of LaConv are predicted from text features, so it can achieve differentiated visual feature learning for different natural language instructions. This property also enable LaConv to perform visual modeling and multi-modal inference in one processing step. Based on LaConv, we can build the unified and end-to-end LaConvNet. LaConvNet gets rid of CNN blocks entirely and directly performs visual reasoning from raw pixels, which greatly differs from existing modular networks for VL tasks. Extensive experiments are conducted on seven benchmarks of three VL tasks. The experimental results not only show the comparable or even better performance of LaConvNet against existing modular multi-modal networks, but also confirm its great superiorities in inference efficiency and model compactness.

**Acknowledgments.** This work was supported by National Key R&D Program of China (No.2022ZD0118201), the National Science Fund for Distinguished Young Scholars (No.62025603), the National Natural Science Foundation of China (No. U21B2037, No. U22B2051, No. 62176222, No. 62176223, No. 62176226, No. 62072386, No. 62072387, No. 62072389, No. 62002305 and No. 62272401), and the Natural Science Foundation of Fujian Province of China (No.2021J01002,

No.2022J06001) and the China Fundamental Research Funds for the Central Universities (Grant No. 20720220068).

## Declarations

- **Funding:** This work was supported by the National Science Fund for Distinguished Young Scholars (No.62025603), the National Natural Science Foundation of China (No. U21B2037, No. 62176222, No. 62176223, No. 62176226, No. 62072386, No. 62072387, No. 62072389, and No. 62002305), Guangdong Basic and Applied Basic Research Foundation (No.2019B1515120049), and the Natural Science Foundation of Fujian Province of China (No.2021J01002).
- **Conflict of interest/Competing interests:** Yongjian Wu is currently the expert researcher and the director of the Youtu Lab, Tencent Co., Ltd. The remaining authors have no relevant financial or non-financial interests to disclose.
- **Ethics approval:** The authors have no relevant ethics approval to disclose.
- **Consent to participate:** All authors agreed to participate in this work and made clear contributions.
- **Consent for publication:** All authors agreed with the content and that all gave explicit consent to submit and that they obtained consent from the responsible authorities at the institute/organization where the work has been carried out.
- **Availability of data and materials:** The datasets analysed during the current study are available in these repositories:  
RefCOCO, RefCOCO+, RefCOCOG and Referit: <https://github.com/lichengunc/refer>;  
Flick30K Entities: [https://github.com/BryanPlummer/flickr30k\\_entities](https://github.com/BryanPlummer/flickr30k_entities);  
CLEVR: <https://cs.stanford.edu/people/jcjohns/clevr/>;  
CLEVR-Ref+: <https://www.cs.jhu.edu/~cxliu/2019/clevr-ref+.html>;  
Visual Genome: <https://visualgenome.org/>.
- **Code availability:** Our code will be released after acceptance.
- **Authors' contributions:** All authors contributed to the study conception and design. Material preparation, data collection and analysis were performed by Gen Luo, Yiyi Zhou, Xiaoshuai Sun and Yue Gao. The first draft of the

manuscript was written by Gen Luo and all authors commented on previous versions of the manuscript. All authors read and approved the final manuscript. More detailed contributions of each author are listed below:

Conceptualization: Gen Luo, Yiyi Zhou and Yongjian Wu; Methodology: Gen Luo, Yiyi Zhou, Xiaoshuai Sun and Yue Gao; Writing - original draft preparation: Gen Luo; Writing - review and editing: Yiyi Zhou, Xiaoshuai Sun, Yongjian Wu, Yue Gao and Rongrong Ji; Supervision: Yiyi Zhou and Rongrong Ji.

## References

- [1] Anderson P, He X, Buehler C, et al (2018) Bottom-up and top-down attention for image captioning and visual question answering. In: Proceedings of the IEEE conference on computer vision and pattern recognition, pp 6077–6086
- [2] Andreas J, Rohrbach M, Darrell T, et al (2016) Neural module networks. In: Proceedings of the IEEE conference on computer vision and pattern recognition, pp 39–48
- [3] Antol S, Agrawal A, Lu J, et al (2015) Vqa: Visual question answering. In: Proceedings of the IEEE international conference on computer vision, pp 2425–2433
- [4] Bhojanapalli S, Yun C, Rawat AS, et al (2020) Low-rank bottleneck in multi-head attention models. In: International Conference on Machine Learning, PMLR, pp 864–873
- [5] Bonath B, Noesselt T, Martinez A, et al (2007) Neural basis of the ventriloquist illusion. *Current Biology* 17(19):1697–1703
- [6] Chen DJ, Jia S, Lo YC, et al (2019) See-through-text grouping for referring image segmentation. In: 2019 IEEE/CVF International Conference on Computer Vision (ICCV), pp 7453–7462, <https://doi.org/10.1109/ICCV.2019.00755>
- [7] Chen YC, Li L, Yu L, et al (2020) Uniter: Universal image-text representation learning.



- In: European conference on computer vision, Springer, pp 104–120
- [8] De Vries H, Strub F, Mary J, et al (2017) Modulating early visual processing by language. In: *Advances in Neural Information Processing Systems*, pp 6594–6604
- [9] Deng J, Yang Z, Chen T, et al (2021) Transvg: End-to-end visual grounding with transformers. *arXiv preprint arXiv:210408541*
- [10] Ding H, Liu C, Wang S, et al (2021) Vision-language transformer and query generation for referring segmentation. In: *Proceedings of the IEEE/CVF International Conference on Computer Vision*, pp 16,321–16,330
- [11] Ding H, Liu C, Wang S, et al (2022) VLT: Vision-language transformer and query generation for referring segmentation. *IEEE Transactions on Pattern Analysis and Machine Intelligence* pp 1–16. <https://doi.org/10.1109/tpami.2022.3217852>, URL <https://doi.org/10.1109%2Ftpami.2022.3217852>
- [12] Dosovitskiy A, Beyer L, Kolesnikov A, et al (2020) An image is worth 16x16 words: Transformers for image recognition at scale. *arXiv preprint arXiv:201011929*
- [13] Escalante HJ, Hernández CA, Gonzalez JA, et al (2010) The segmented and annotated iapr tc-12 benchmark. *Computer vision and image understanding* 114(4):419–428
- [14] Feng G, Hu Z, Zhang L, et al (2021) Encoder fusion network with co-attention embedding for referring image segmentation. <https://doi.org/10.48550/ARXIV.2105.01839>, URL <https://arxiv.org/abs/2105.01839>
- [15] Gan Z, Chen YC, Li L, et al (2020) Large-scale adversarial training for vision-and-language representation learning. In: *NeurIPS*
- [16] Gao P, Li H, Li S, et al (2018) Question-guided hybrid convolution for visual question answering. In: *Proceedings of the European Conference on Computer Vision (ECCV)*, pp 469–485
- [17] Goyal Y, Khot T, Summers-Stay D, et al (2017) Making the v in vqa matter: Elevating the role of image understanding in visual question answering. In: *Proceedings of the IEEE Conference on Computer Vision and Pattern Recognition*, pp 6904–6913
- [18] He K, Zhang X, Ren S, et al (2016) Deep residual learning for image recognition. In: *Proceedings of the IEEE conference on computer vision and pattern recognition*, pp 770–778
- [19] He K, Gkioxari G, Dollár P, et al (2017) Mask r-cnn. In: *Proceedings of the IEEE international conference on computer vision*, pp 2961–2969
- [20] He K, Chen X, Xie S, et al (2022) Masked autoencoders are scalable vision learners. In: *Proceedings of the IEEE/CVF Conference on Computer Vision and Pattern Recognition*, pp 16,000–16,009
- [21] Hu R, Singh A (2021) Unit: Multimodal multitask learning with a unified transformer. In: *Proceedings of the IEEE/CVF International Conference on Computer Vision*, pp 1439–1449
- [22] Hu R, Andreas J, Rohrbach M, et al (2017) Learning to reason: End-to-end module networks for visual question answering. In: *Proceedings of the IEEE International Conference on Computer Vision*, pp 804–813
- [23] Hu R, Rohrbach M, Andreas J, et al (2017) Modeling relationships in referential expressions with compositional modular networks. In: *CVPR*
- [24] Hu R, Andreas J, Darrell T, et al (2018) Explainable neural computation via stack neural module networks. In: *Proceedings of the European conference on computer vision (ECCV)*, pp 53–69
- [25] Hu Z, Feng G, Sun J, et al (2020) Bi-directional relationship inferring network



- for referring image segmentation. In: 2020 IEEE/CVF Conference on Computer Vision and Pattern Recognition (CVPR), pp 4423–4432, <https://doi.org/10.1109/CVPR42600.2020.00448>
- [26] Huang B, Lian D, Luo W, et al (2021) Look before you leap: Learning landmark features for one-stage visual grounding. In: Proceedings of the IEEE/CVF Conference on Computer Vision and Pattern Recognition, pp 16,888–16,897
- [27] Huang S, Hui T, Liu S, et al (2020) Referring image segmentation via cross-modal progressive comprehension. <https://doi.org/10.48550/ARXIV.2010.00514>, URL <https://arxiv.org/abs/2010.00514>
- [28] Hudson D, Manning CD (2019) Learning by abstraction: The neural state machine. In: Advances in Neural Information Processing Systems, pp 5903–5916
- [29] Hudson DA, Manning CD (2018) Compositional attention networks for machine reasoning. In: International Conference on Learning Representations
- [30] Hudson DA, Manning CD (2019) Gqa: A new dataset for real-world visual reasoning and compositional question answering. In: Proceedings of the IEEE Conference on Computer Vision and Pattern Recognition, pp 6700–6709
- [31] Hui T, Liu S, Huang S, et al (2020) Linguistic structure guided context modeling for referring image segmentation. <https://doi.org/10.48550/ARXIV.2010.00515>, URL <https://arxiv.org/abs/2010.00515>
- [32] Jin L, Luo G, Zhou Y, et al (2023) Refclip: A universal teacher for weakly supervised referring expression comprehension. In: Proceedings of the IEEE/CVF Conference on Computer Vision and Pattern Recognition, pp 2681–2690
- [33] Jing Y, Kong T, Wang W, et al (2021) Locate then segment: A strong pipeline for referring image segmentation. <https://doi.org/10.48550/ARXIV.2103.16284>, URL <https://arxiv.org/abs/2103.16284>
- [34] Johnson J, Hariharan B, van der Maaten L, et al (2017) Clevr: A diagnostic dataset for compositional language and elementary visual reasoning. In: Proceedings of the IEEE Conference on Computer Vision and Pattern Recognition, pp 2901–2910
- [35] Johnson J, Hariharan B, Van Der Maaten L, et al (2017) Inferring and executing programs for visual reasoning. In: Proceedings of the IEEE International Conference on Computer Vision, pp 2989–2998
- [36] Kazemzadeh S, Ordonez V, Matten M, et al (2014) Referitgame: Referring to objects in photographs of natural scenes. In: EMNLP
- [37] Kim JH, Jun J, Zhang BT (2018) Bilinear attention networks. arXiv preprint arXiv:180507932
- [38] Kim N, Kim D, Lan C, et al (2022) Restr: Convolution-free referring image segmentation using transformers. <https://doi.org/10.48550/ARXIV.2203.16768>, URL <https://arxiv.org/abs/2203.16768>
- [39] Kim W, Son B, Kim I (2021) Vilt: Vision-and-language transformer without convolution or region supervision. arXiv preprint arXiv:210203334
- [40] Kingma DP, Ba J (2014) Adam: A method for stochastic optimization. arXiv preprint arXiv:1412.6980
- [41] Krishna R, Zhu Y, Groth O, et al (2017) Visual genome: Connecting language and vision using crowdsourced dense image annotations. International journal of computer vision 123(1):32–73
- [42] Krizhevsky A, Sutskever I, Hinton GE (2012) Imagenet classification with deep convolutional neural networks. In: Advances in neural information processing systems, pp 1097–1105

- [43] Li J, Li D, Savarese S, et al (2023) Blip-2: Bootstrapping language-image pre-training with frozen image encoders and large language models. arXiv preprint arXiv:230112597
- [44] Lin TY, Maire M, Belongie S, et al (2014) Microsoft coco: Common objects in context. In: European conference on computer vision, Springer, pp 740–755
- [45] Liu C, Lin Z, Shen X, et al (2017) Recurrent multimodal interaction for referring image segmentation. In: Proceedings of the IEEE International Conference on Computer Vision, pp 1271–1280
- [46] Liu C, Ding H, Jiang X (2023) Gres: Generalized referring expression segmentation. In: Proceedings of the IEEE/CVF Conference on Computer Vision and Pattern Recognition, pp 23,592–23,601
- [47] Liu D, Zhang H, Wu F, et al (2019) Learning to assemble neural module tree networks for visual grounding. In: ICCV
- [48] Liu R, Liu C, Bai Y, et al (2019) Clevr-ref+: Diagnosing visual reasoning with referring expressions. In: Proceedings of the IEEE Conference on Computer Vision and Pattern Recognition, pp 4185–4194
- [49] Liu S, Hui T, Huang S, et al (2021) Cross-modal progressive comprehension for referring segmentation. <https://doi.org/10.48550/ARXIV.2105.07175>, URL <https://arxiv.org/abs/2105.07175>
- [50] Liu X, Wang Z, Shao J, et al (2019) Improving referring expression grounding with cross-modal attention-guided erasing. In: Proceedings of the IEEE/CVF Conference on Computer Vision and Pattern Recognition, pp 1950–1959
- [51] Liu Z, Lin Y, Cao Y, et al (2021) Swin transformer: Hierarchical vision transformer using shifted windows. In: Proceedings of the IEEE/CVF international conference on computer vision, pp 10,012–10,022
- [52] Lu J, Clark C, Zellers R, et al (2022) Unified-io: A unified model for vision, language, and multi-modal tasks. arXiv preprint arXiv:220608916
- [53] Luo G, Zhou Y, Ji R, et al (2020) Cascade grouped attention network for referring expression segmentation. In: Proceedings of the 28th ACM International Conference on Multimedia. Association for Computing Machinery, New York, NY, USA, MM '20, p 1274–1282, <https://doi.org/10.1145/3394171.3414006>, URL <https://doi.org/10.1145/3394171.3414006>
- [54] Luo G, Zhou Y, Sun X, et al (2020) Multi-task collaborative network for joint referring expression comprehension and segmentation. In: Proceedings of the IEEE/CVF Conference on Computer Vision and Pattern Recognition (CVPR)
- [55] Luo G, Zhou Y, Sun X, et al (2022) Towards lightweight transformer via group-wise transformation for vision-and-language tasks. IEEE Transactions on Image Processing 31:3386–3398
- [56] Mao J, Huang J, Toshev A, et al (2016) Generation and comprehension of unambiguous object descriptions. In: CVPR
- [57] Mao J, Gan C, Kohli P, et al (2019) The neuro-symbolic concept learner: Interpreting scenes, words, and sentences from natural supervision. arXiv preprint arXiv:190412584
- [58] Mascharka D, Tran P, Soklaski R, et al (2018) Transparency by design: Closing the gap between performance and interpretability in visual reasoning. In: Proceedings of the IEEE conference on computer vision and pattern recognition, pp 4942–4950
- [59] McGurk H, MacDonald J (1976) Hearing lips and seeing voices. Nature 264(5588):746–748
- [60] Morency LP, Mihalcea R, Doshi P (2011) Towards multimodal sentiment analysis: Harvesting opinions from the web. In: Proceedings of the 13th international conference on multimodal interfaces, pp 169–176

- [61] Nagaraja VK, Morariu VI, Davis LS (2016) Modeling context between objects for referring expression understanding. In: ECCV
- [62] Nguyen DK, Goswami V, Chen X (2020) Revisiting modulated convolutions for visual counting and beyond. arXiv preprint arXiv:200411883
- [63] Pennington J, Socher R, Manning CD (2014) Glove: Global vectors for word representation. In: Proceedings of the 2014 conference on empirical methods in natural language processing (EMNLP), pp 1532–1543
- [64] Perez E, Strub F, de Vries H, et al (2018) Film: Visual reasoning with a general conditioning layer. In: AAAI
- [65] Plummer BA, Wang L, Cervantes CM, et al (2015) Flickr30k entities: Collecting region-to-phrase correspondences for richer image-to-sentence models. In: Proceedings of the IEEE international conference on computer vision, pp 2641–2649
- [66] Poria S, Cambria E, Gelbukh A (2015) Deep convolutional neural network textual features and multiple kernel learning for utterance-level multimodal sentiment analysis. In: Proceedings of the 2015 conference on empirical methods in natural language processing, pp 2539–2544
- [67] Qiu H, Li H, Wu Q, et al (2020) Language-aware fine-grained object representation for referring expression comprehension. In: Proceedings of the 28th ACM International Conference on Multimedia, pp 4171–4180
- [68] Redmon J, Farhadi A (2018) Yolov3: An incremental improvement. arXiv preprint arXiv:180402767
- [69] Ren S, He K, Girshick R, et al (2015) Faster r-cnn: Towards real-time object detection with region proposal networks. arXiv preprint arXiv:150601497
- [70] Sadhu A, Chen K, Nevatia R (2019) Zero-shot grounding of objects from natural language queries. In: ICCV
- [71] Santoro A, Raposo D, Barrett DG, et al (2017) A simple neural network module for relational reasoning. In: Advances in neural information processing systems, pp 4967–4976
- [72] Shams L, Kamitani Y, Shimojo S (2002) Visual illusion induced by sound. *Cognitive brain research* 14(1):147–152
- [73] Shrestha R, Kafle K, Kanan C (2019) Answer them all! toward universal visual question answering models. In: Proceedings of the IEEE conference on computer vision and pattern recognition, pp 10,472–10,481
- [74] Stein BE, Stanford TR (2008) Multisensory integration: current issues from the perspective of the single neuron. *Nature reviews neuroscience* 9(4):255–266
- [75] Suarez J, Johnson J, Li FF (2018) Ddrprog: A clevr differentiable dynamic reasoning programmer. arXiv preprint arXiv:180311361
- [76] Sun J, Luo G, Zhou Y, et al (2023) Refteacher: A strong baseline for semi-supervised referring expression comprehension. In: Proceedings of the IEEE/CVF Conference on Computer Vision and Pattern Recognition, pp 19,144–19,154
- [77] Sun M, Xiao J, Lim EG (2021) Iterative shrinking for referring expression grounding using deep reinforcement learning. In: Proceedings of the IEEE/CVF Conference on Computer Vision and Pattern Recognition, pp 14,060–14,069
- [78] Tan M, Le Q (2019) Efficientnet: Rethinking model scaling for convolutional neural networks. In: International conference on machine learning, PMLR, pp 6105–6114
- [79] Vaswani A, Shazeer N, Parmar N, et al (2017) Attention is all you need. In: Advances in neural information processing systems, pp 5998–6008
- [80] Wang L, Li Y, Huang J, et al (2018) Learning two-branch neural networks for image-text matching tasks. *IEEE Transactions on*

Pattern Analysis and Machine Intelligence  
41(2):394–407

- [81] Wang Z, Lu Y, Li Q, et al (2021) Cris: Clip-driven referring image segmentation. <https://doi.org/10.48550/ARXIV.2111.15174>, URL <https://arxiv.org/abs/2111.15174>
- [82] Wang Z, Yu J, Yu AW, et al (2021) Simvlm: Simple visual language model pretraining with weak supervision. arXiv preprint arXiv:210810904
- [83] Xu H, Yan M, Li C, et al (2021) E2e-rlp: end-to-end vision-language pre-training enhanced by visual learning. arXiv preprint arXiv:210601804
- [84] Yang S, Xia M, Li G, et al (2021) Bottom-up shift and reasoning for referring image segmentation. In: 2021 IEEE/CVF Conference on Computer Vision and Pattern Recognition (CVPR), pp 11,261–11,270, <https://doi.org/10.1109/CVPR46437.2021.01111>
- [85] Yang Z, He X, Gao J, et al (2016) Stacked attention networks for image question answering. In: Proceedings of the IEEE conference on computer vision and pattern recognition, pp 21–29
- [86] Yang Z, Gong B, Wang L, et al (2019) A fast and accurate one-stage approach to visual grounding. In: Proceedings of the IEEE/CVF International Conference on Computer Vision, pp 4683–4693
- [87] Yang Z, Chen T, Wang L, et al (2020) Improving one-stage visual grounding by recursive sub-query construction. arXiv preprint arXiv:200801059
- [88] Yang Z, Wang J, Tang Y, et al (2021) Lavt: Language-aware vision transformer for referring image segmentation. <https://doi.org/10.48550/ARXIV.2112.02244>, URL <https://arxiv.org/abs/2112.02244>
- [89] Ye L, Rochan M, Liu Z, et al (2019) Cross-modal self-attention network for referring image segmentation. <https://doi.org/10.48550/ARXIV.1904.04745>, URL <https://arxiv.org/abs/1904.04745>
- [90] Yi K, Wu J, Gan C, et al (2018) Neural-symbolic vqa: Disentangling reasoning from vision and language understanding. In: Advances in neural information processing systems, pp 1031–1042
- [91] Yu F, Tang J, Yin W, et al (2021) Ernie-vil: Knowledge enhanced vision-language representations through scene graphs. In: Proceedings of the AAAI Conference on Artificial Intelligence, pp 3208–3216
- [92] Yu L, Lin Z, Shen X, et al (2018) Mattnet: Modular attention network for referring expression comprehension. In: Proceedings of the IEEE Conference on Computer Vision and Pattern Recognition, pp 1307–1315
- [93] Yu Z, Yu J, Xiang C, et al (2018) Rethinking diversified and discriminative proposal generation for visual grounding. arXiv preprint arXiv:180503508
- [94] Yu Z, Yu J, Cui Y, et al (2019) Deep modular co-attention networks for visual question answering. In: Proceedings of the IEEE/CVF Conference on Computer Vision and Pattern Recognition, pp 6281–6290
- [95] Zadeh A, Zellers R, Pincus E, et al (2016) Mosi: multimodal corpus of sentiment intensity and subjectivity analysis in online opinion videos. arXiv preprint arXiv:160606259
- [96] Zhang T, Tseng HY, Jiang L, et al (2020) Text as neural operator: Image manipulation by text instruction. arXiv preprint arXiv:200804556
- [97] Zhou Y, Ji R, Sun X, et al (2019) Plenty is plague: Fine-grained learning for visual question answering. IEEE transactions on pattern analysis and machine intelligence 44(2):697–709
- [98] Zhou Y, Ji R, Luo G, et al (2021) A real-time global inference network for one-stage referring expression comprehension. IEEE TNNLS

- [99] Zhou Y, Ren T, Zhu C, et al (2021) Trar: Routing the attention spans in transformer for visual question answering. In: Proceedings of the IEEE/CVF International Conference on Computer Vision, pp 2074–2084